Turbine Blades for Reusable Liquid Rocket Engines (LRE) – Numerical Fatigue Life Investigation

Mateusz T. Gulczyński, Jörg R. Riccius*, Evgeny B. Zametaev*, Robson H. S. Hahn*, Günther Waxenegger-Wilfing*, Jan C. Deeken**, Michael Oschwald****

***German Aerospace Center (DLR) – Institute of Space Propulsion**
****German Aerospace Center (DLR) – Institute of Space Propulsion, RWTH Aachen University**
Im Langen Grund, 74239 Hardthausen am Kocher, Germany

Corresponding author contact: Mateusz.Gulczynski@dlr.de

Abstract—**Reusability of LREs in Europe is increasingly attracting the attention of scientific community and industry with leading projects such as THEMIS, CALLISTO (reusable demonstrators for vertical take-off and landing (VTVL)) and Ariane Next – all powered by the reusable cryogenic Oxygen/Methane (LOX/LCH4) engine "Prometheus". To enable further expansion and cost-effectiveness of the reusability technology for future liquid rocket engines (LREs), research on critical engine components such as turbopumps is crucial. Therefore, within our research we focus on the turbine blade investigation for reusable LRE applications including high cycle fatigue (HCF) and low cycle fatigue (LCF). Validation of defined applied analytical and numerical techniques is established through the Liquid Upper stage deMonstrator ENgine (LUMEN)'s, developed at DLR Lamplodshausen for enhanced expertise in the complete cycle operation for various engine applications, as well as to empower validation studies of the operational conditions to which turbopump components, such as turbine blades, are subjected.**

Turbine blades are exposed to large thermo-mechanical cyclic strains emerging from an increased temperature driving gas combined with a fast start-up sequence as well as a large rotational speed – essential for acquiring high performance and structural mass efficiency for LREs. Therefore, in addition to bending & torsion as well as thermal gradient and centrifugal forces, it is critical to consider creep effects in durability studies.

To forecast the turbine blade fatigue life, analytical (0-D) and numerical approaches for a selected test case are studied. Within the proposed method, a BLISK is assessed for the most severe loading condition considering HCF load by a modified Goodman method, along with a Coffin-Manson based approach for LCF contribution. Each operational cycle under constant maximum loading condition is applied to study the creep effect. As a result, an enhanced fatigue life prediction method including both creep and fatigue conditions for a turbine blade is obtained.

TABLE OF CONTENTS

1. INTRODUCTION

The turbopumps of a Liquid Rocket Engine (LRE) plays a vital role in obtaining a high specific impulse and high thrust-to-weight ratio. To determine the reusability capacity of the LRE's turbopump, it is essential to evaluate the main stresses in the blades to estimate the permissible margins for the High Cycle Fatigue (HCF) and the Low Cycle Fatigue (LCF) life of the turbine. At elevated rotational speed, indispensable to achieve a high power-to-weight ratio, a large tensile prestressing of turbine blades may be observed. Over and above that, circumferential flow variations of the turbine driving gas, ejected from the stator row(s) of the turbopump, is the source of a severe HCF loading of turbine blades. As reported in Space Shuttle Main Engine (SSME) with full admission turbines, as well as in case of a more recently developed fuel turbopump of the Japanese LE-5B engine with partial admission turbines, the fatigue life related failures and cracks in turbine blades can be identified already during the pre-development and pre-qualification phases [1], [2], [3], [4]. On that account, within the presented paper, the generally applicable numerical method is proposed to evaluate a fatigue life of the turbine blades under severe loading conditions. As a validation case, a Liquid Upper Stage deMonstrator ENgine (LUMEN) is employed – an expander-bleed breadboard engine in the 25kN thrust class, working on a mixture of liquid oxygen (LOX) and methane. It enables a complete engine cycle operation and validation studies for a given operational conditions to which turbopump components are subjected. The LUMEN demonstrator is located at test bench P8.3 in DLR Lampoldshausen, Institute of Space Propulsion.

2023 IEEE Aerospace Conference | 978-1-6654-9032-0/23/$31.00 ©2023 IEEE | DOI: 10.1109/AERO55745.2023.10115912

2. (0-D) STRUCTURAL ANALYSIS OF THE TURBOPUMP'S BLADES

The turbopump rotor blades and guide vanes are subjected to gas-dynamic loads resulting from the pressure distribution across the blade airfoils. In addition, at increased rotating speed, the blades masses may induce significant transverse loads along the curvilinear paths which results from gyroscopic moments and centrifugal transverse forces [5]. The main loads acting on the turbine blades can be therefore divided to: static and dynamic loads – arising from the flowing medium acting on the blade profile, mass loads induced by centrifugal force, as well as loads triggered by elastic vibrations of the blades and the entire rotor. During operations, these loads translate into the following main stresses [6]:

- Tensile stresses – resulting from centrifugal forces of the rotating blade mass;
- Bending stresses – induced by the flowing medium acting on the blade profile, as well as stresses resulting from centrifugal forces of the rotating blade mass along with stresses caused by transverse vibrations of the blade;
- Tangential stresses – resulting from torsional moments force induced by the flowing medium acting on the blade profile, in addition to torsional moments of the mass forces acting on the blade, and torsional vibration of the blades active part.

In the Figure 1, the main geometrical parameters of the LUMEN turbine blade are presented. In the following sub-sections, the analytical approach for calculating TB main loads, including: rotational, gas pressure, mechanical is presented [1], [6], [7], [8], [9], [10], [11], [12], [13], [14].

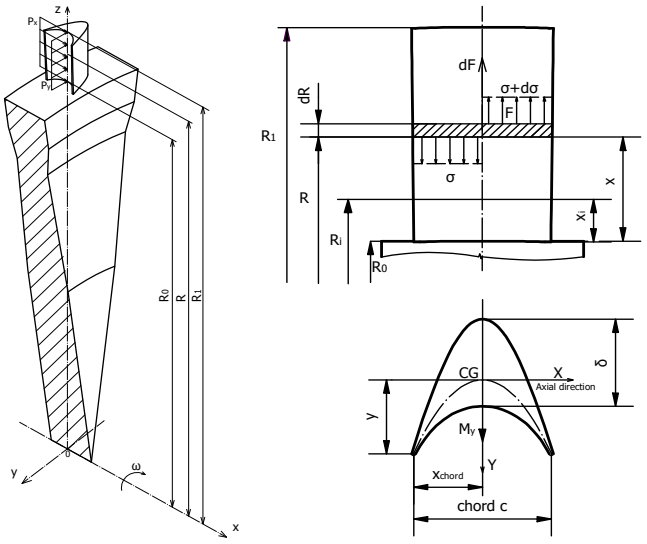

Figure 1 Schematic of the LUMEN TP with a blade geometry ("R_0" – root radius, "R_1" – tip radius, "R_{mean}" – blade centroid radius) (M. T. Gulczyński et al.)

Tensile Loads Acting on the Blade Resulting from Centrifugal Forces of the Rotating Blade Mass

For a rotor that spins with an angular velocity "ω", a differential centrifugal force acting on the blade element of length dR is calculated in accordance with equation (1):

$$F_i = \frac{\omega^2}{g}\int_{x_i}^{l} \gamma A(R_0 + x)dx \tag{1}$$

The highest centrifugal force is calculated for the cross-section at the root of the blade, at "R_0", with a following equation:

$$F_0 = \frac{\omega^2}{g}\int_{0}^{l} \gamma A(R_0 + x)dx \tag{2}$$

Consequently, the centrifugal stresses at the given radius of the blade are estimated as highlighted in equation (3):

$$\sigma_R = \frac{\omega^2}{gA_i}\int_{x_i}^{l} \gamma A(R_0 + x)dx = \frac{\gamma\omega^2}{2g}\frac{\pi(R_1^2 - R_i^2)}{\pi} \tag{3}$$

where "$\pi(R_1^2 - R_i^2) = \Phi$" represents a cross-section of the blade airfoil through which the flowing medium passes. Based on equation (3), the admissible stresses "k_r" acting on the blade material are estimated. In dependence on the blade material, operating conditions (e.g. temperature, flowing medium) as well as admissible stress factor, the elastic growth of the blade is calculated:

$$\Delta l = \frac{\gamma\omega^2}{2gE}\int_{R_0}^{R_1} (R_1^2 - r_i^2)\mathrm{d}r_i = \frac{\gamma\omega^2}{6gE}R_1^3\left(2 - 3\frac{R_o}{R_1} + \frac{R_o^3}{R_1^3}\right) \tag{4}$$

Finally, the blade tensile loads resulting from centrifugal forces of the rotating blade mass are calculated using a tabular method [6], where a blade is divided into smaller sections.

Bending Moments Induced by Fluid Medium's Pressure and The Centrifugal Loads

The fluid medium passing through the blades generates dynamic force and force induced by the pressure difference between a front and rear part of the blade. The force components, denoted by "P_x" and "P_y", as highlighted in Figure 1, are determined from the equations (5).

$$\begin{cases} P_x = \frac{2\pi r}{i}\left[(p_1 - p_2) + \frac{1}{g}(\gamma_1 c_{la}^2 - \gamma_2 c_{2a}^2)\right] \\ P_y = \frac{2\pi r}{ig}\left[\gamma_1 c_{1u}(c_{\mathrm{Lu}} - u) + \gamma_2 c_{2a}(c_{2u} + u)\right] \end{cases} \tag{5}$$

The bending moments are subsequently calculated with equations (6):

$$\begin{cases} M_{\mathrm{xg}} = \int_{z_0}^{l} P_y (z - z_0) dz = P_y \frac{(l-z_0)^2}{2} \\ M_{\mathrm{yg}} = \int_{z_0}^{l} P_x (z - z_0) dz = P_x \frac{(l-z_0)^2}{2} \end{cases} \quad (6)$$

As in case of tensile loads calculations, the bending moments are calculated using a tabular method, where the blade is sectioned along the height, similarly to what was presented in the Figure 1.

To calculate the total bending moment about the x-axis in section "i" induced by centrifugal loads, the following equation (7) is applied:

$$\begin{cases} M_{x_{bending}} = \frac{\gamma}{g} \omega^2 \int_{R_i}^{R_1} A(yR_i - y_i R) dR \\ M_{y_{bending}} = \frac{\gamma}{g} \omega^2 \int_{R_i}^{R_1} A(x - x_i) \mathrm{RdR} \end{cases} \quad (7)$$

Bending Stresses in the Outermost Layers of the Blade

To determine the bending stresses in the outermost layers of the blade, a center of gravity and a moment of inertia for the given blade profile is calculated. The geometrical parameters, as highlighted in Figure 1, together with velocity triangles, as shown in Figure 2, are applied for turbine stress calculation. The blade profile is approximated with geometrical figures applied to a blade cross-section, which allows for a quick estimation of the stress components. As shown in Figure 2, the moments of inertia of the LUMEN's impulse turbine blade are calculated in accordance with a Steiner's parallel axis theorem:

$$\begin{cases} I_x = I_{x_0} - Aa^2 \\ I_y = I_{y_0} - Ab^2 \\ I_{xy} = I_{x_0 y_0} - Aab \end{cases} \quad (8)$$

where "A" represents the cross-sectional area of the blade, and "a" and "b" are the distances between given axes.

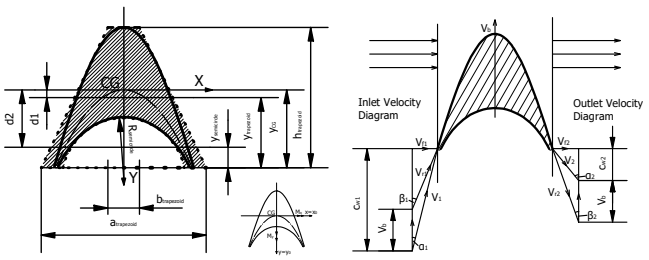

(a) **(b)**

Figure 2 Schematic cross-sections of the LUMEN impulse turbine blade profile, highlighting: (a) blade geometry with central axis system with bending moments acting on the blade profile; (b) velocity triangles in front of and behind the blade (M. T. Gulczyński et al.)

The centre of gravity for the LUMEN impulse turbine profile is calculated as follows (9):

$$\begin{cases} d_1 = y_{CG} - y_{trapezoid} \\ d_2 = y_{CG} - y_{semicircle} \\ S_{x_{ITB}} = \left[\left(\frac{(a+b)h}{2}\right)(-d_1)\right] - \left[\left(\frac{\pi R^2}{2}\right)(-d_2)\right] \\ A_{area} = \frac{(a+b)h}{2} - \frac{\pi R^2}{2} \\ y = \frac{S_x}{A_{area}} \end{cases} \quad (9)$$

which leads to equation (10) for centre of gravity.

$$CG = y_{CB} + y \quad (10)$$

The turbine moments of inertia about central principal axes are calculated equations (11) for an impulse turbine type.

$$\begin{cases} I_x = I_{x_0} - Aa^2 = \left[\frac{(a+3b)h^3}{12} - \frac{\pi R^4}{8}\right] - Aa^2 \\ I_y = I_{y_0} - Ab^2 = \left[\frac{(a+b)(a^2+b^2)h}{48} + \left(\frac{(a+b)h}{2}(d_1 + CB)^2\right] - \left[\frac{\pi R^4}{8} + \frac{\pi R^2}{2}(d_2 + CB)^2\right] - Ab^2 \end{cases} \quad (11)$$

As impulse turbine blades are symmetric, the "x=0" and "$M_{x_0} = M_x$" and "$M_{y_0} = -M_y$" therefore, the bending stress at any arbitrary point of the section is determined by:

$$\sigma_{gas\ bending} = \frac{M_{x_0}}{I_{x_0}} y \quad (12)$$

A change in the angular momentum of the gas in the tangential direction results in the force that generates a useful torque and a gas bending moment in the axial direction. Consequently, a gas bending stress amounts to the tensile stress – in the leading and trailing edge, and compressive stress – on the suction side of the blade. The leading or trailing edge of the root section is often where the highest stress is located [1], [7], [8], [15]. For the calculations of gas bending and centrifugal stresses, the velocity triangles schematic is used as highlighted in Figure 2(b).

For the considered partial admission turbine – the gas bending stress is reduced to zero in the non-admission parts of the turbine, where stress amplitude $\sigma_{a,0D}$ obtained by this 0D method is half of the max. gas bending stress:

$$\sigma_{a,0D} = \frac{\sigma_{gb,max,0D}}{2} \quad (13)$$

The mean stress $\sigma_{m,0D}$ obtained by this 0D method is the sum of the centrifugal stress and the stress amplitude:

$$\sigma_{m,0D} = \sigma_{c,0D} + \sigma_{a,0D} \quad (14)$$

The main geometric parameters along with operating conditions applied to the calculations are presented in the following sections (Table 2, Table 3) [16], [17].

3. LUMEN'S TURBOPUMP DESIGN CHARACTERISTICS

As opposed to traditionally used pump fluid for cooling, LUMEN turbopump employs oil lubricated bearings, which improves life expectancy as well as increases the adaptivity of the system. This design choice facilitates investigation of the turbopump components, including turbine blades and pumps, without additional need for a major system modification. The LUMEN's turbopump consists of a single-stage and single-rotor pressure-compounded impulse turbine. Both – Fuel Turbopump (FTP) and Oxidizer Turbopump (OTP) share the similar design, where no static pressure drop occur and there is no expansion. The design utilizes only one stage (one stationary nozzle) followed by a row of rotating blades, what helps in retaining the gas flow velocity, and thus the kinetic energy at entrance and exhaust. The rotor dynamic analysis is realized with a DLR in-house tool "ROTAN", where parameter variation are performed to estimate the critical speed of OTP and FTP, along with solution sensitivity evaluation to the respective parameter (impeller and turbine weight, bearing and shaft diameter, shaft sections length etc.) [18]. The schematic representation of the LUMEN's architecture along with a cross-section of the LOx and LNG turbopump is presented in Figure 3.

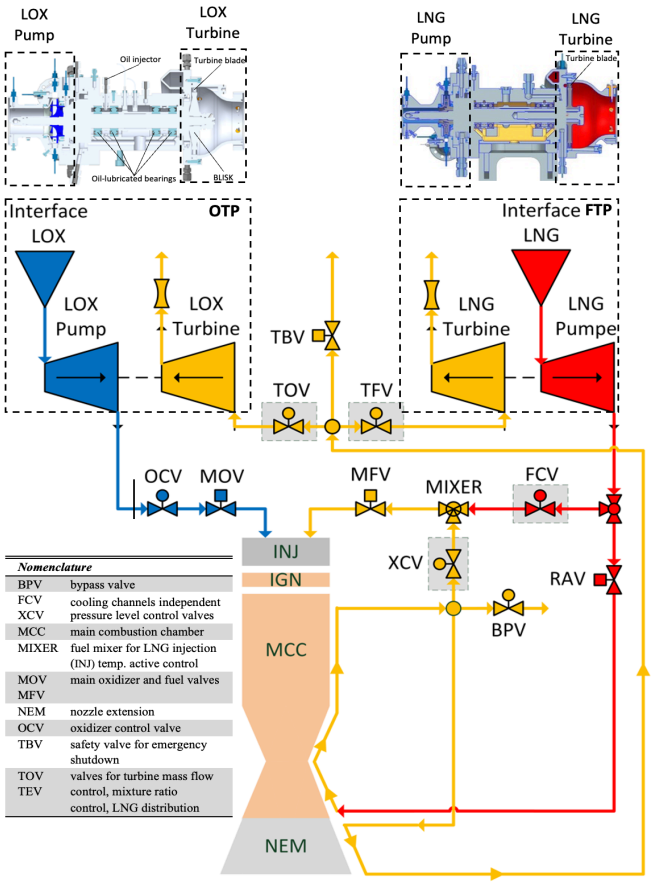

Figure 3 LUMEN demonstrator engine schematic representation combining LOx and LNG Turbopump cross-sections. (partially adapted from [14], [19], [20]) (M. T. Gulczyński et al.)

LUMEN Turbopumps Operational Parameters

The study on fuel and oxygen turbopump starts with preliminary fluid dynamics analysis, where based on the entrance conditions obtained from the flow path analysis, the turbine exit gas pressure is established. The remaining variables (partially presented in Table 1): velocity ratio, rotational speed of the turbine, diameter, specific speed, and admission fraction, are calculated subsequently and utilized to evaluate the turbine efficiency.

Table 1 LUMEN's turbopump operating conditions

Description	Min	Max	Unit
$T_{injection,LNG}$	190	-	K
$T_{turbine,inlet}$	$f(p_{turbine,inlet})$	550	K
$T_{wall,chamber}$	-	900	K
$\eta_{turbine}$	-	η_{max}	-
$p_{turbine,inlet}$	30	-	bar
$p_{pump,LNG}$	-	150	bar

Based on before mentioned values, the turbine blade driving force is calculated along with remaining input factors, crucial for the HCF and LCF analysis [1]. The diagram below (Figure 4) highlights a transient model property applied to FEM analysis. The pressure and temperature (at a total inlet condition) are measured before the stator nozzle resulting in the maximum gas temperature level in the system. Once the medium has left a stator, the pressure and temperature decrease due to expansion, resulting in a static pressure and temperature. Owing to gas dynamics, the rotor blades will be mostly exposed to static temperature however, at some locations the shock structure will stagnate the gas, increasing its temperature to approximately initial value.

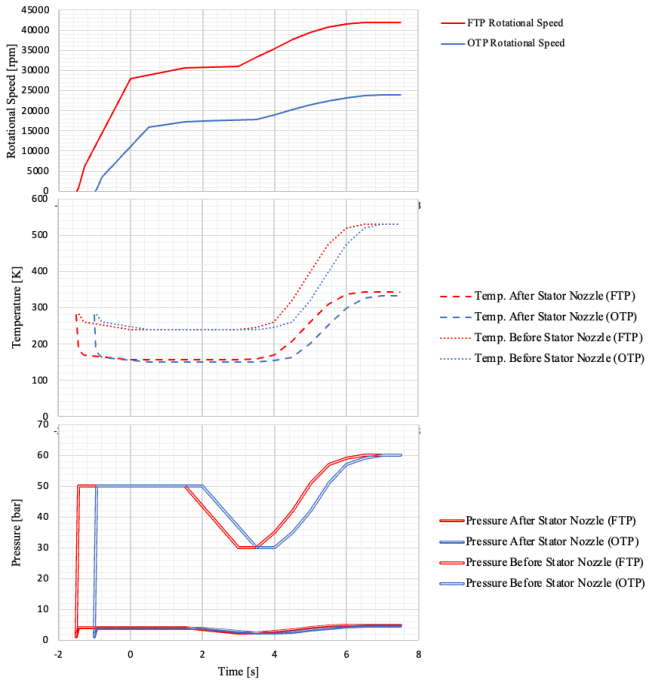

Figure 4 LUMEN's turbopump operational sequence (M. T. Gulczyński et al.)

Although commonly a total temperature after expansion is lower due to friction losses in the system, in case of LUMEN the decrease of a total outlet temperature is negligible throughout all operational conditions. Therefore, the structural temperature of both stator and rotor is ceaselessly comparable. In case of the LUMEN turbopump, operational sequence starts with a chill-down of the pump followed by a downstream pipeline chill-down. Subsequently, the turbopump starts-up until the nominal operational speed is reached. Thereafter, it operates at constant speed until shut-down and full-stop at the end of operational time. The change in blade film coefficient and temperature is primary at nominal operational step. During a chill-down phase (around 300s), the decrease of enthalpy in the turbine blade is also insignificant. Following the chill-down phase, the shaft region is exposed to a minimum temperature of 280K – therefore, the BLISK won't be subjected to cryogenic temperature. In diagram below (Figure 5), an example of the static temperature distribution on the blade surface was presented for a corresponding operational condition to LUMEN. The surface temperature depends on the evaluated load point and the time in the transient analysis.

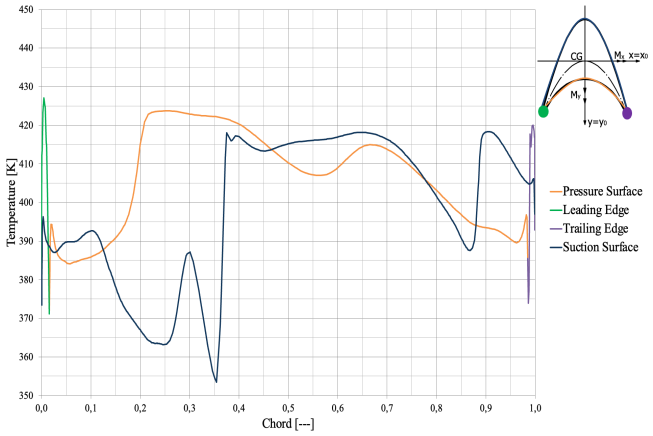

Figure 5 Example of static temperature distribution on the blade surface at operational conditions analogous to LUMEN (M. T. Gulczyński et al.)

LUMEN's Turbine Blade Design Features

The LUMEN's turbopump partial admission turbine blade design choice arises from the admission degree evaluation and a trade-off study between the blade geometry, turbine size, along with a required stator exhaust velocity and the high cycle fatigue loads. The evolution of radial clearance ratio and blade height ratio is assessed considering an admission degree. An increased admission degree of the LUMEN's supersonic impulse turbine results in a uniform flow through the rotor and reduction of the main losses of its parameters. Concurrently, the fixed meridional diameter and radial gap influences the blade height which has to be reduced, what generates more losses related to leakage at radial clearance [9].

4. Structural 3D Finite Element Analysis Method

To estimate a critical life of the LUMEN's turbine blades, the FEM method is developed incorporating a quasi-stationary structural 3D Finite Element Model for the HCF part, along with a transient model to account for LCF effects. The presented approach is versatile and enables estimation of a critical life of any turbine blades, including a reusability potential evaluation. Furthermore, the proposed method is transferable to large-scale engine's components of a similar design. Within presented FEM analysis, three load steps (LS1 to LS3) provide sufficient input data for the post-processing HCF and LCF analysis:

• LS1: Transient thermal loading (including start-up phase, nominal operation and a shut-down of an engine).

• LS2: Additional spin loading (modelling centrifugal forces under elevated temperature and therefore, representing the loading of the turbine blade in the non- admission sections of the turbine).

• LS3: Additional (circumferential) blade driving load in the admission sections of the turbine (caused by the turbine driving gas, emitted by the stator row).

For the post processing HCF analysis, the maximum principal stresses at the maximum loading point for load steps LS2 and LS3 of the 3D Finite Element analysis are relevant, whereas in case of the LCF, load step LS1 is essential. The key geometric parameters of referenced LUMEN's turbine blades are presented in Table 2.

Table 2 LUMEN's OTP and FTP input data

Description	**Parameter**	**Value**	**Unit**
Mass of the blade	m	0.0017	kg
Radius of the blade centroid	R_{mean}	0.0635	m
Number of blade driving jets	$n_{stat\ (OTP)}$ $n_{stat\ (FTP)}$	3 5	-
Fillet radius (transition between the disk and the blade)	r_{fillet}	0.005	m
Blade height	h_{OTP} h_{FTP}	0.0093 0.0097	m
Number of blades	n_{blades}	65	-
Input for the calculation of the blade camber angle	β_{1r} β_{2r}	69 18	°
Maximum blade thickness	t_{OTP} t_{FTP}	0.00370 0.00406	m
Chord length (OTP &FTP)	c	0.009	m
Tangential component of entering stream (whirl velocity)	C_{w1}	246.9	m/s
Corresponding value at exit of the moving blade	C_{w2}	201.9	m/s
Mass flow rate	$\dot{m}$	1.046	kg/s
Admission degree	Θ_{OTP} Θ_{FTP}	0.229 0.356	
Density	$\gamma_{Inconel\ 718}$	8.19	g/cm^3

5. POST-PROCESSING ANALYSIS

As part of the turbine blade HCF analysis's initial stage, the maximum principal stresses of the highest loaded point of the turbine blade are extracted from load steps LS_2 and LS_3 of the structural 3D Finite Element analysis. Thereafter, the mean stress "$\sigma_{m,3D}$" (as mean value of the max. principal stresses of the two 3D FE analysis load steps LS_2 and LS_3) and stress amplitude "$\sigma_{a,3D}$" (as half of the difference of the maximum principal stresses, extracted from the two considered 3D FE analysis load steps LS_3 and LS_2) are calculated. As previously stated at the end of Section 2, the 0D analysis (based on the beam theory) can be alternatively applied to determine the loads. Finally, the following equation determines the number of cycles until failure "N_f" (as suggested in reference [21]):

$$N_f = \sqrt[B']{\frac{\sigma_a}{A'\left(1-\frac{\sigma_m}{C'}\right)}} \tag{15}$$

Contrary to the original Goodman equation, with a stress amplitude "σ_a" being normalised by "σ_{N_f}" at fully reversed loading conditions "R=-1", "$\sigma_m = 0$" and the mean stress being normalized by the failure stress at constant loading conditions "R=1", "$\sigma_a = 0$" to the ultimate tensile stress; within the herewith demonstrated modified Goodman equation (15), the "σ_{N_f}" is substituted by the stress amplitude "σ_f"at which the assessed turbine blade material fails after "N_f" cycles at a given mean stress level ("$\sigma_m \neq 0$") and "σ_{UTS}" is replaced by a parameter C'.

Turbine Blade's Material Parameters & Loading Conditions

The LUMEN turbopumps operate in a temperature ranging from cryogenic up to driving gas temperature of 500K. On that account, the material chosen for the turbine blade is Inconel 718, which offers unique properties for structures exposed to high pressure and extreme temperatures in a range of -240°C up to 700°C. Furthermore, a protective oxide layer provides a significant amount of resistance to oxidation, thereby increasing turbopump reusability potential. The structural worst-case (recorded at the location of the blade leading edge) is established by evaluating the blade loading conditions for nine operating points for both LUMEN's Oxygen and Fuel turbine. Correspondingly with this data, the operating conditions with the highest amplitude and the shortest fatigue life are analysed. The main loading conditions for both turbopumps are highlighted in Table 3.

Table 3 Structural-worst-case operating point blade loading conditions of the LUMEN's OTP and FTP

Loading conditions	Parameter	Value	Unit
Rotational speed OTP	ω_{OTP}	2806	rad/sec
	ω_{FTP}	5395	
Turbine driving gas temperature	T_{OTP}	488.36	K
	T_{FTP}	487.4	
Single blade loading (in circumferential direction)	$F_{single,OTP}$	49,37	N
	$F_{single,FTP}$	31.97	

To allow for flexibility of the model (e.g. follow-on Finite Element analysis of the remaining operating points of the LUMEN TP blade) a temperature dependent modulus of elasticity (as seen in Figure 6) and a temperature dependent thermal expansion coefficient (as may be seen in Figure 7) are particularize as an input of the structural 3D Finite Element analysis.

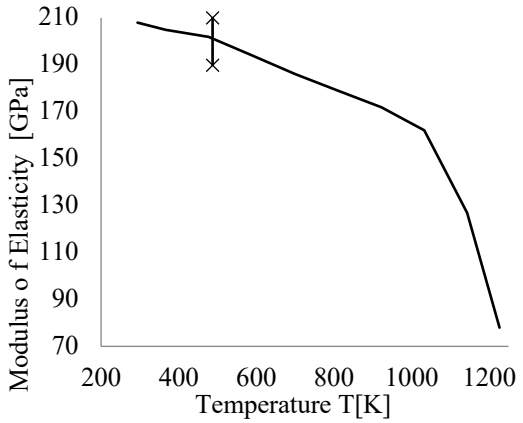

Figure 6 Temperature dependency of the modulus of elasticity (M. T. Gulczyński et al.)

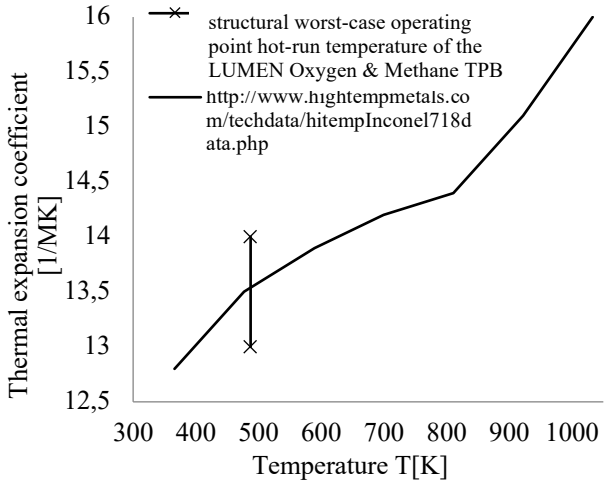

Figure 7 Thermal expansion coefficient of Inconel 718 at the structural worst-case hot-run operating point of the LUMEN TP (M. T. Gulczyński et al.)

As highlighted above, a temperature dependent material parameters – both: for modelling elasto- plasticity as well as for creep were used for the structural Finite Element analyses. The HCF analysis parameters of Inconel 718 (summarized in Table 4), are available for ambient temperature only (in accordance with [21]). (Temperature independent parameters "$\varrho_{Inc718} = 8192\,\frac{kg}{m^3}$", "ν=0.31" applied)

Table 4 Parameters, used for the HCF analysis

HCF analysis parameter	Value	Unit
A'	7160	MPa
B'	-0.1872	-
C'	1154	MPa

FEM Boundary Conditions and Mesh Characteristic

On the left- hand side of Figure 8, the transient structural boundary conditions applied to the 3D Finite Element model of the LUMEN OTP and FTP blade are presented. As may be observed in Figure 8(a), the yellow faces represent symmetry and convective boundary conditions, where the total temperature of the turbine driving gas, in the local coordinate system of the blade, is of maximum 500K. A blade driving force of "F_{single} = 49.37N" (in case of the OTP as an example) is distributed as a constant pressure on the surface highlighted with a red colour (always acting in the direction normal to the surface).

The 3D model is discretized with a tetrahedral or brick shape elements – 3D 10-Node Tetrahedral Structural, 3D 20-Node Structural Solid elements. The non-linear model of both OTP and FTP includes a maximum element size of 0.8mm, where for the fitting and edge areas, at which maximum stress and strain values are obtained, the mesh is refined resulting in an 0.05mm and 0.02mm element size respectively for OTP, along with 0.1mm and 0.012mm for FTP. The step size approach for mesh refinement of the blade-hub transition is used. The meshing reveals a total of 577881 elements and 858714 nodes for OTP, and 196386 elements and 293313 nodes for FTP. The Finite Element mesh, used for the 3D analysis of the LUMEN TP blades is shown in Figure 8(b). The gradual zoom levels – A(2:1) and B(3:1) – demonstrate the refinement of the Finite Element mesh in the vicinity of the maximum loading point of the model (the transition of the blade to the disk at the leading edge of the blade).

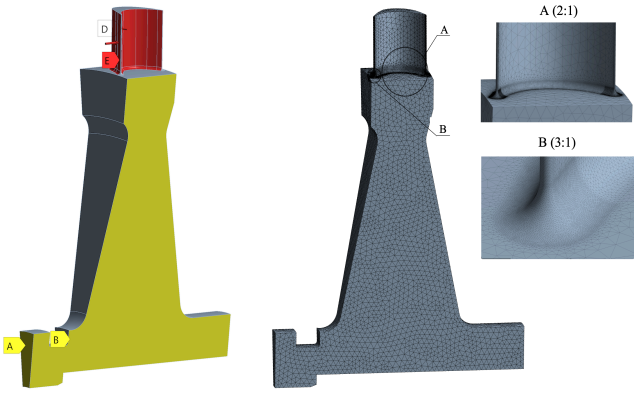

(a) **(b)**

Figure 8 (a) Applied boundary conditions (b) Finite Element Mesh as used for the structural 3D FEA of the LUMEN Oxygen TP blade and related disk section (M. T. Gulczyński et al.)

Transient Structural 3D Finite Element Analysis Results

To account for the LCF effects, a fully transient thermal analysis is applied to the Finite Element model. In Figure 9 the results for a minimum principal total strain are highlighted, the minimum principal total strain was found to be lower than the plasticity limit. Due to moderate operating temperature (of max 500K), the radial creep deformation of the turbine blade at the end of the full loading cycle was found to be insignificant. Conclusively, the creep does not contribute to the failure of the LUMEN turbine blade under given loading conditions.

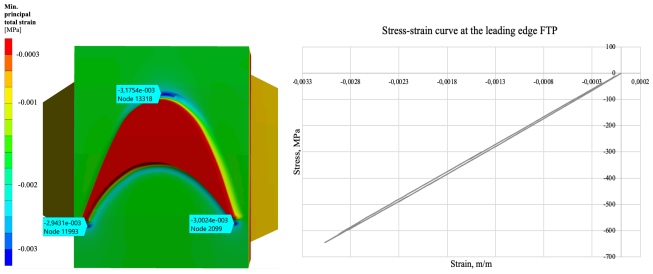

Figure 9 Min. principal total strain, obtained by fully transient thermal Finite Element analysis of the LUMEN FTP blade (M. T. Gulczyński et al.)

The maximum principal stress fields, obtained by load steps LS2 (combined thermal and centrifugal loading) and LS3 (combined thermal, centrifugal and gas bending loading) of the 3D FE analysis of the LUMEN TP blade are presented in Figure 10 and Figure 11 respectively (and for both type of turbopumps).

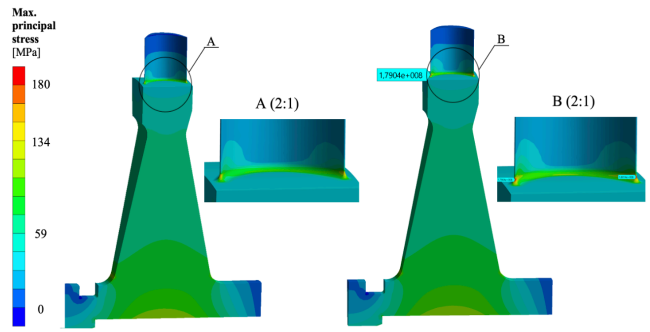

Figure 10 Max. principal stress fields, obtained by load steps LS2 (a) and LS3 (b) of the 3D Finite Element analysis of the LUMEN Oxygen TP blade (M. T. Gulczyński et al.)

As it may be observed from the numerical analysis, for both cases LS_2 and LS_3, the max. principal stresses are recorded in the proximity of the turbine blade root on the pressure and the suction side of the blade. The stress is decreasing towards the tip – which is characteristic of the tensile load. The centrifugal stress is dependent on the blade material mass, blade length and the rotational speed.

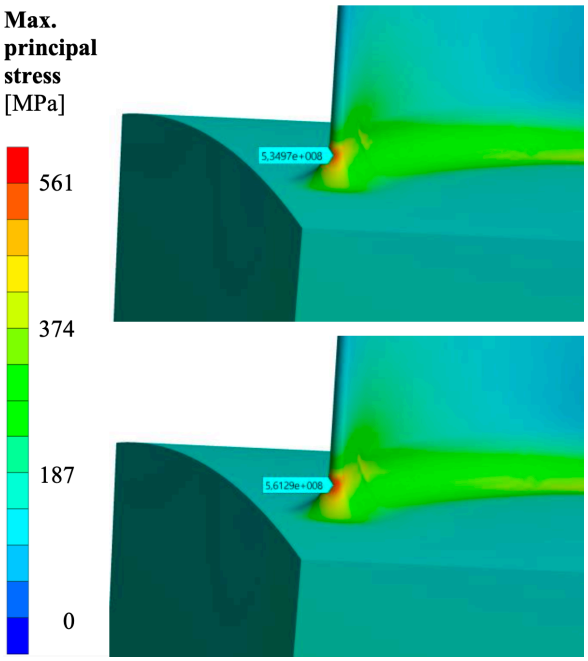

Figure 11 Max. principal stress fields, obtained by load steps LS2 and LS3 of the 3D Finite Element analysis of the LUMEN Fuel TP blade (M. T. Gulczyński et al.)

In Figure 12 and Figure 13, the max. principal stresses for transient loading in function of time recorded for 475 substeps are shown, combined with a cross-section with max. principal stress fields for load step 2 (LS_2) and load step 3 (LS_3). As indicated, for the evaluated operating point, the max. principal stresses at the leading edge and trailing edge are of the similar magnitude, what is expected for a partial admission turbine.

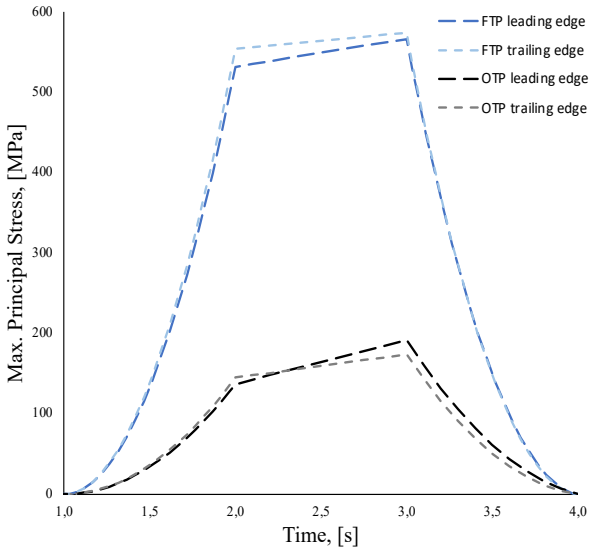

Figure 12 Maximum Principal Stresses for the LUMEN OTP & FTP blade at leading and trailing edge for load step 2 – LS2 and load step 3 – LS3 (M. T. Gulczyński et al.)

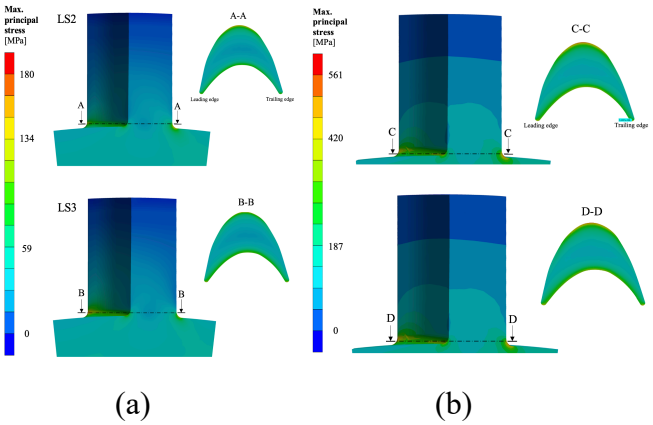

Figure 13 Maximum Principal Stresses for the LUMEN LOx (a) and Methane (b) TP blade at leading and trailing edge for load step 2 – LS2 and load step 3 – LS3 (M. T. Gulczyński et al.)

For the numerical analysis, the min. principal stress is equal to "$\sigma_{c,3D\ (OTP)} = 139MPa$" as obtained by the combination of centrifugal and thermal loading – LS_2. In case of combined thermal, centrifugal & max. gas bending loading – LS_3, the maximum principal stress is equal to "$\sigma_{c,3D\ (OTP)} + \sigma_{gb,max,3D\ (OTP)} = 179MPa$". In comparison, within 0D analysis calculated with equations presented in section 2 and under equivalent loading conditions as well as with similar material parameters, the centrifugal and gas bending stress corresponds to "$\sigma_{c,0D\ (OTP)} = 195.4MPa$" and "$\sigma_{gb,max,0D\ (OTP)} = 38.29MPa$". The comparison of the numerical and analytical 0D results for OTP is summarized in Table 5.

Table 5 Structural-worst-case operating point blade loading conditions of the LUMEN Oxygen TP

Nomenclature	Parameter	3D FE analysis	0D beam theory	Unit	0D value / 3D value
Cyclic stress	σ_{cyclic}	40.4	38.3	MPa	5%
Stress amplitude	σ_a	20.2	19.15	MPa	5%
Mean stress	σ_m	158.9	214.55	MPa	26%

The further comparison of analytical and numerical methods for FTP, presented in Table 6, utilizes a 0D calculation approach introduced in publication [7]. This was conducted for additional accuracy evaluation of the analytical method previously proposed.

Table 6 Structural-worst-case operating point blade loading conditions of the LUMEN Methane TP (0D calculations applied in accordance with methodology presented in [1] and [7] for accuracy comparison)

Nomenclature	Parameter	3D FE analysis	0D beam theory	Unit	0D value / 3D value
Cyclic stress	σ_{cyclic}	26	18	MPa	30%
Stress amplitude	σ_a	13	9	MPa	30%
Mean stress	σ_m	549	396	MPa	28%

Results Outline

The OTP stresses obtained from the 0D beam theory suggested in section 2 were found to be approximately 26% higher than the stresses received through the 3D Finite Element Analysis. In comparison, the stresses calculated with previously developed methods [7], differs from FEM by 28%. The inaccuracy in calculations between 0D and FEM, could be on account of stresses being calculated in radial direction of the turbine (equaling to the height direction of the turbine blade) for former, in contrast to max. principal stresses extracted for latter.

The mean stress (green and blue line) and the stress amplitude (violet line) as obtained by the 3D Finite Element analysis in relation to the test data given in Reference [21] (blue circles) used for fitting the HCF analysis parameters A', B' and C' (as given in Table 4) is visualized in Figure 14. The large gap between the (violet) stress amplitude line and the (blue) circles, indicates that the HCF analysis of the operating point of the considered turbine blade requires a large extrapolation of experimental HCF data. In order to visualize the HCF analysis according to equation (19), HCF life iso lines for 100 Mcycles, 10 Gcyles and 1 Tcycle were calculated by this equation and additionally included in Figure 14 (combined with Haigh diagram for Inconel 718).

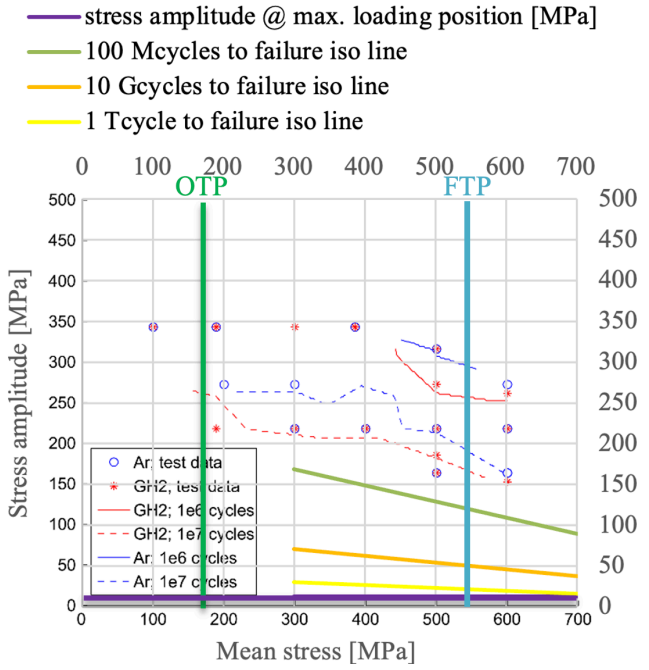

Figure 14 Visualization of the structural-worst-case-operating point of the LUMEN Oxygen and Methane TP blade (crossing point of the green and the violet line) in relation to HCF test data (blue circles). OTP and FTP vertical lines represents the mean stress value at maximum loading position (M. T. Gulczyński et al.)

Due to the low stress amplitude of just 20 MPa, the HCF life of the LUMEN TP blades, as predicted by equation (6), is as high as $N_f = 17$ trillion cycles before failure for OTP and 17 trillion cycles for FTP. To increase the performance and efficiency of the engine, a higher temperature in the turbomachinery component is inevitable. Therefore, it is especially important for the future reusable applications, that the turbomachinery components are evaluated considering the operating temperature. The assessed turbopump material operates within the hot-run temperature range of approximately 500K – where for Inconel 718 the yield strength within this temperature range is as high as "$\sigma_{yield,\ Inconel718\ atT=500\ K}$ =1100MPa" [22]. Therefore, the life reduction due to thermal loading is found to have an insignificant influence.

6. Summary and Outlook

Within presented paper, two structural analysis methods were compared: 0D analysis – based on the beam theory, and a transient 3D Finite Element method. The analytical approach was found to be in an acceptable margin with the respective results, obtained by the 3D FE analysis. The post-processing transient HCF/LCF analysis, based on the max. principal stress values of the above-mentioned 3D Finite Element analysis, resulted in a fatigue life of 17 trillion cycles before failure for Oxygen Turbopump, and 13 trillion cycles to failure for a Methane Turbopump. Furthermore, for the considered reference turbine blade, the HCF (at the leading edge of the reference turbine blade) seems to be dominant in relation to LCF failure (at the trailing edge of the turbine blade). Due to the relatively moderate hot-run temperature (500K) of the reference turbine blade, creep-caused failure is fully negligible.

The foreseen improvements of the presented methods will include further developed transient analysis and a damped vibration of the turbine blade in the non-admission sections of the turbine. Furthermore, an extended fatigue life analysis with implementation of a damage accumulation method presented in [23], [24], for improved accuracy of the LCF models is envisage. For the post-processing HCF/LCF evaluation, additional tests are foreseen outside LUMEN demonstrator, where LCF effects at increased operating temperatures can be validated. What's more, the study of the turbopump life reduction due to elevated temperatures is envisioned, which shall prove the versatility of the hereby presented methods when evaluating turbopumps working in wider spectrum conditions, including large scale turbopump turbines operating within higher temperature range. The lessening blade's life influenced by effects such as multiaxial fatigue – combined HCF and LCF ([25]), creep or corrosion, will be further evaluated with developed models for different engine applications.

Acknowledgements

The project leading to this paper has received funding from the European Union's Horizon 2020 research & innovation programme under the Marie Skłodowska-Curie grant agreement No 860956.

REFERENCES

[1] J. R. Riccius, E. B. Zametaev, M. T. Gulczyński, and R. H. S. Hahn, "NUMERICAL LRE TURBINE BLADE FATIGUE LIFE ANALYSIS TAKING INTO ACCOUNT PARTIAL ADMISSION EFFECTS," 2022.

[2] H. Lee, "Space Shuttle Main Engine high pressure fuel turbopump turbine blade cracking," *NASA Tech. Memo.*, vol. 3190, no. NASA TM-100327, 1987.

[3] N. Nagao, H. Nanri, K. Okita, Y. Ishizu, S. Yabuki, and S. Kohno, "The Modified Fuel Turbopump of 2nd stage engine for H3 launch vehicle," pp. 1–7, doi: 10.13009/EUCASS2017-189.

[4] R. E. Biggs, *Space Shuttle Main Engine: The First Twenty Years and Beyond*, Volume 29. 1980.

[5] Z. Dżygadło, M. Łyżwiński, J. Otyś, S. Szceciński, and R. Wiatrek, *Napędy Lotnicze - Zespoły Wirnikowe Silników Turbinowych*. Wydawnictwo Komunikacji i Łączności, 1982.

[6] J. Lipka, *Wytrzymalosc Maszyn Wirnikowych*. Wyd. Naukowo-Techniczne Warszawa, 1967.

[7] M. T. Gulczyński *et al.*, "Numerical Turbine Blade Fatigue Life Analysis for Reusable Liquid Rocket Engines (LREs) Applications," 2022, no. 9TH EUROPEAN CONFERENCE FOR AERONAUTICS AND SPACE SCIENCES (EUCASS), doi: 10.13009/EUCASS2022-6150.

[8] Г. Г. Гахун and . и др (сост.), *КОНСТРУКЦИЯ И ПРОЕКТИРОВАНИЕ ЖИДКОСТНЫХ РАКЕТНЫХ ДВИГАТЕЛЕЙ*. Москва Машиностроение, 1989.

[9] Robson H. S. Hahn, Jan C. Deeken, Tobias Traudt, Michael Oschwald, Stefan Schlechtriem, and Hideyo Negishi, "LUMEN Turbopump - Preliminary Design of Supersonic Turbine,", 2019.

[10] N. A. and S. Administration, "NASA SP-8110 Liquid Rocket Engine Turbines," 1974.

[11] H. I. H. Saravanamuttoo, H. Cohen, G. F. C. Rogers, P. V. Straznicky, and A. C. Nix, *Gas Turbine Theory Gas Turbine Theory*. 2017.

[12] Jack L. Kerrebrock, *Aircraft Engines and Gas Turbines, Second Edition*. The MIT Press, 1992.

[13] M. T. Gulczynski *et al.*, "RLV applications: challenges and benefits of novel technologies for sustainable main stages," Oct. 2021. [Online]. Available: https://elib.dlr.de/148758/

[14] R. H. S. Hahn, M. T. Gulczyński, E. Kurudzija, K. Dresia, G. Waxenegger-Wilfing, and J. Deeken, "LUMEN Evolution for Lunar Lander Propulsion"

[15] W. Zhang, *Failure characteristics analysis and fault diagnosis for liquid rocket engines*. 2016. doi: 10.1007/978-3-662-49254-3.

[16] R. Kumar et al., "Thermo-mechanical analysis and estimation of turbine blade tip clearance of a small gas turbine engine under transient operating conditions," *Appl. Therm. Eng.*, vol. 179, 2020, doi: 10.1016/j.applthermaleng.2020.115700.

[17] R. I. Thamizh, R. Velmurugan, and R. Jayagandhan, "Finite element analysis of metal matrix composite blade," *IOP Conf. Ser. Mater. Sci. Eng.*, vol. 152, no. 1, 2016, doi: 10.1088/1757-899X/152/1/012008.

[18] T. Traudt et al., "LUMEN Turbopump - Design and Manufacturing of the LUMEN LOX and LNG Turbopump components," 2019.

[19] T. Traudt *et al.*, "LIQUID UPPER STAGE DEMONSTRATOR ENGINE (LUMEN): COMPONENT TEST RESULTS AND PROJECT PROGRESS," in *Space Propulsion Conference 2022*, 2022, no. SP2022_00362.

[20] J. Deeken, M. Oschwald, and S. Schlechtriem, "LUMEN DEMONSTRATOR – PROJECT OVERVIEW," no. March, 2021.

[21] M. Bruchhausen *et al.*, "Impact of hydrogen on the high cycle fatigue behaviour of Inconel 718 in asymmetric push-pull mode at room temperature," *Int. J. Fatigue*, vol. 70, pp. 137–145, 2015, doi: 10.1016/j.ijfatigue.2014.09.005.

[22] Y. Zhang *et al.*, "Microstructures and properties of high-entropy alloys," *Prog. Mater. Sci.*, vol. 61, no. November 2013, pp. 1–93, 2014, doi: 10.1016/j.pmatsci.2013.10.001.

[23] M. T. Gulczyński, J. R. Riccius, G. Waxenegger-wilfing, J. C. Deeken, and M. Oschwald, "Numerical Fatigue Life Analysis of Combustion Chamber Walls for Future Reusable Liquid Rocket Engines (LREs) Applications," 2022, no. SP2022.

[24] M. T. Gulczyński, J. R. Riccius, G. Waxenegger-wilfing, J. C. Deeken, and M. Oschwald, "Combustion Chamber Fatigue Life Analysis for Reusable Liquid Rocket Engines (LREs)," 2023, AIAA SciTech Forum 2023, pp. 1-16.

[25] J. R. Riccius, E. B. Zametaev, and L. J. Souverein, "HCF, LCF and creep life analysis of a generic LRE turbine blade," *AIAA Sci. Technol. Forum Expo. AIAA SciTech Forum 2022*, pp. 1–10, 2022, doi: 10.2514/6.2022-0796.

BIOGRAPHY

Mateusz T. Gulczyński *is a Research Scientist in Rocket Engine Systems Department at the Institute of Space Propulsion at German Aerospace Center (DLR) and a PhD Student for Reusable Space Propulsion Systems at RWTH Aachen University. His area of activity enfolds rocket engine design and operation with a specific focus on methods for fatigue life estimation of highly loaded rocket engine components into low order tools for rocket engine cycle modeling.*

Jörg R. Riccius *received his Ph.D. degree in civil engineering from KIT Karlsruhe, boosted by a 2-year post-doc position at the department of aeronautics of the Imperial College London. He is the technical leader of the Structures team (inside the Rocket Propulsion department) at the German Aerospace Center (DLR). His research is focused on method development for (thermal and structural) FE and fatigue life analyses of liquid rocket engine (LRE) components including validation by dedicated LRE sub-component tests.*

Evgeny B. Zametaev *received his engineering education from the MINT (Moscow Physic Technic Institute) in 1983. Till 2001 he worked at the CADB (Chemical Automatic Design Bureau) in Voronezh, Russia, as a leader of the FE analyses group. In 1997-1998, he participated in the Russian Teams in the Space-Shuttle-Nozzle-Projects. Since 2001 he has worked at the DLR Institute of Space Propulsion, Department of Rocket Propulsion Technology, Structure Group. His research is focused on structure and thermal FE analyses of the Rocket engines: turbopump, chamber, nozzle and other elements of the LRE.*

Robson H. S. Hahn *graduated in Physics at Estate University of Mato Grosso do Sul (UEMS) in 2007, received his Master Degree in Space Propulsion by Technological Institute of Aeronautics (ITA) and Moscow State Aviation University (MAI) in 2010 on topics of Liquid Propellant Rocket Engines. Work in Research and development of LPRE at Institute of Aeronautics and Space (IAE), from 2008 to 2015 and from 2013 to 2015 was manager of combustion system for L75 project. Since November of 2015 is working at German Aerospace Center as part of System Analysis group as well as in the LUMEN Project, especially in the Turbopump development and test front as well as in the Transient analysis system.*

Günther Waxenegger-Wilfing *received his Ph.D. degree in theoretical physics from the University of Vienna. He is currently a professor for aerospace computer science at the University of Würzburg and at the same time head of the system analysis and control research group at the Institute of Space Propulsion at the German Aerospace Center (DLR). His main research interest is the application of machine learning and artificial Intelligence methods to problems in aerospace with a specific focus on rocket engine design and control as well as autonomous spacecraft operation.*

Jan C. Deeken *received his Diploma degree in mechanical engineering from RWTH Aachen University in 2007 and joined DLR Institute of Space Propulsion in Lampoldshausen the same year. He received his Ph.D. title for his work on porous injectors for high-pressure rocket combustion chambers in 2014 from Stuttgart University. Since 2020 he is the acting department head of the newly found rocket engine system department at the Institute of Space Propulsion. Together with his coworkers in three research groups he is working on topics ranging from thrust chamber design, turbopump design, system analysis and control for cryogenic liquid rocket engines. In 2022 he took over the Chair of Space Propulsion at the Institute for Jet Propulsion and Turbomachinery at RWTH Aachen University.*

Michael Oschwald *is Coordinator for Rocket Propulsion at the Institute of Space Propulsion at the German Aerospace Center (DLR) and professor for Space Propulsion of the RWTH Aachen University. His fields of activity cover all aspects of rocket engine design and operation with a specific focus on cryogenic propulsion. His department at DLR has a long heritage in experimental investigations of high pressure combustion, heat transfer, combustion instabilities, and expansion nozzles. In parallel to the experimental work numerical tools are developed in his department to predict the behavior of rocket engines and their components.*